Acta Astronautica 127 (2016) 103–111

Contents lists available at ScienceDirect

Acta Astronautica

journal homepage: www.elsevier.com/locate/aa

The NEOTωIST mission (Near-Earth Object Transfer of angular momentum spin test)

Line Drube [a,*], Alan W. Harris [a], Kilian Engel [b], Albert Falke [b], Ulrich Johann [b], Siegfried Eggl [c], Juan L. Cano [d], Javier Martín Ávila [d], Stephen R. Schwartz [e], Patrick Michel [e]

[a] Institute of Planetary Research, German Aerospace Center (DLR), Rutherfordstr. 2, 12489 Berlin, Germany
[b] Airbus DS, Claude-Dornier-Str., 88090 Immenstaad, Germany
[c] IMCCE, Observatoire de Paris, 77 Avenue Denfert-Rochereau, 75014 Paris, France
[d] DEIMOS Space S.L.U., Ronda de Poniente 19, 28760 Tres Cantos, Spain
[e] CNRS, Observatoire de la Côte d'Azur, Boulevard de l'Observatoire, 06300 Nice, France

ARTICLE INFO

Article history:
Received 9 September 2015
Received in revised form
5 April 2016
Accepted 7 May 2016
Available online 25 May 2016

Keywords:
Near-Earth Objects
Asteroids
Impact hazard
Asteroid deflection
Planetary defense
Kinetic impactor

ABSTRACT

We present a concept for a kinetic impactor demonstration mission, which intends to change the spin rate of a previously-visited asteroid, in this case 25143 Itokawa. The mission would determine the efficiency of momentum transfer during an impact, and help mature the technology required for a kinetic impactor mission, both of which are important precursors for a future space mission to deflect an asteroid by collisional means in an emergency situation. Most demonstration mission concepts to date are based on changing an asteroid's heliocentric orbit and require a reconnaissance spacecraft to measure the very small orbital perturbation due to the impact. Our concept is a low-cost alternative, requiring only a single launch.

Taking Itokawa as an example, an estimate of the order of magnitude of the change in the spin period, δP, with such a mission results in δP of ~4 min (0.5%), which could be detectable by Earth-based observatories.

Our preliminary study found that a mission concept in which an impactor produces a change in an asteroid's spin rate could provide valuable information for the assessment of the viability of the kinetic-impactor asteroid deflection concept. Furthermore, the data gained from the mission would be of great benefit for our understanding of the collisional evolution of asteroids and the physics behind crater and ejecta-cloud development.

1. Introduction

The impact of comet Shoemaker-Levy 9 on Jupiter in 1994 was of a magnitude that would have killed most species had the same object impacted on Earth. The Shoemaker-Levy 9 event was a stark reminder that collisions between small bodies in the Solar System and planets continue to shape the surfaces of the latter and pose a real danger to our civilization on Earth. Efforts were subsequently increased to detect near-Earth objects (NEOs) and derive their orbits, in order to calculate their impact probabilities. Two decades later the million-inhabitant Russian city of Chelyabinsk experienced the largest asteroid impact on Earth in a hundred years, when a previously undetected asteroid with a diameter of about 18 m exploded some 25–30 km above the ground. The shockwave from the atmospheric explosion shattered windows in several thousand buildings and caused more than a thousand people to seek medical attention, mainly due to cuts from flying glass pieces.

While the Chelyabinsk event has highlighted the need to broaden the NEO search programs to detect small NEOs, it also serves as a further reminder of the Earth's vulnerability to NEO impacts in general. For objects larger than about 50 m deflection may become a politically-favored course of action. In that case, knowledge of when an asteroid will collide with Earth has to be followed up with knowledge of how to prevent the impact. Many ideas regarding methods of asteroid deflection have been considered in recent years. The option currently favored by most experts for the most probable scenarios is the kinetic impactor, in which a spacecraft is flown into the asteroid at high velocity to

Abbreviations: DSNR, Detection Signal-to-Noise Ratio; FoM, Figure of Merit; NEO, Near-Earth Object; NEOTωIST, Near-Earth Object Transfer of angular momentum ($=\omega^* I$) Spin Test; LPF, Lisa Pathfinder Propulsion module

* Corresponding author.
E-mail addresses: Line.Drube@dlr.de (L. Drube), Alan.Harris@dlr.de (A.W. Harris), kilian.engel@airbus.com (K. Engel), albert.falke@airbus.com (A. Falke), ulrich.johann@airbus.com (U. Johann), Siegfried.Eggl@obspm.fr (S. Eggl), juan-luis.cano@deimos-space.com (J.L. Cano), javier.martin@deimos-space.com (J.M. Ávila), srs@oca.eu (S.R. Schwartz), michelp@oca.eu (P. Michel).

http://dx.doi.org/10.1016/j.actaastro.2016.05.009
0094-5765/

change its orbit slightly. The change has to be just enough so that the threatening asteroid arrives at the predicted impact point earlier or later than Earth, thereby making a close flyby instead of an impact. However, there are a number of unknown factors that prevent accurate predictions of an asteroid's response to the impact of a spacecraft, as the kinetic-impactor technique has never been tested on a real NEO. Computer simulations of impacts of spacecraft into asteroids lack experimental data to allow realistic testing and calibration of the code. Another challenge is achieving the accuracy required of the impacting spacecraft's guidance, control and navigation system, which has to act autonomously in the final approach phase.

A demonstration deflection space mission is essential if we want to be confident of our ability to deflect asteroids by collisional means in an emergency impact-hazard situation.

The NEOShield [1] consortium consisted of 13 institutes, universities and industrial partners from 6 countries, with the objective of addressing the global issue of preventing a hazardous NEO impact on Earth. The project was funded by the European Commission's Seventh Framework Program. A major aim of NEOShield was to design technically and financially realistic deflection demonstration missions, which was continued into the NEOShield-2 project. Here we present a low-budget kinetic-impactor demonstration mission concept called NEOTωIST (Near-Earth Object Transfer of angular momentum ($=\omega^* I$) Spin Test).

2. Mission concept

The NEOTωIST concept is a kinetic impactor demonstration mission that can be performed with a lower budget than most other suggested kinetic-impactor demonstration missions and still provide the possibility to validate impact models and deflection predictions. Most demonstration mission concepts to date are based on changing an asteroid's heliocentric orbit and require a second spacecraft to follow the asteroid for some time after the impact to measure the very small orbital perturbation due to the impact. In contrast, our concept is to measure the efficiency of the momentum transfer by impacting an already well-characterized asteroid at some distance from the rotation axis, thereby transferring angular momentum to it (see Fig. 1). The impact will cause the asteroid's rotational period to change, which can be observed from Earth by measuring the asteroid's rotationally induced lightcurve. Lengthy reconnaissance phases before and after the impact requiring a second spacecraft are therefore not essential.

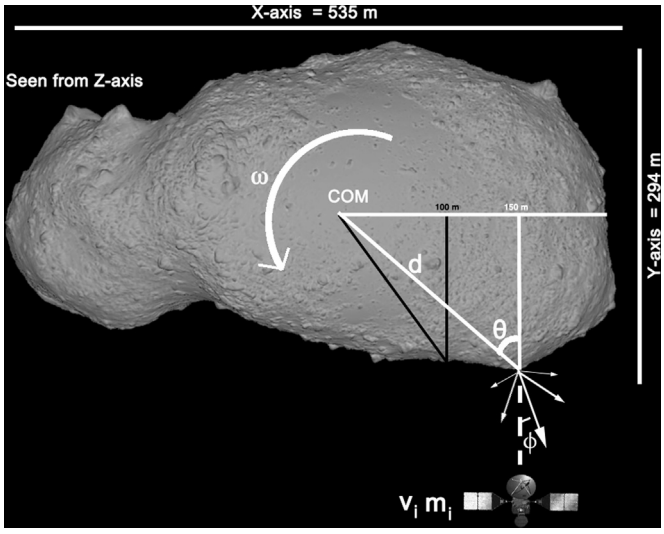

Fig. 1. Impact geometry. A kinetic impactor impacts off-center on Itokawa thereby changing its rotational period. Itokawa's dimensions are $535 \times 294 \times 209\ m^3$ [2] and it rotates around the *Z*-axis perpendicular to the image. The lower part of the image is called the eastern side. Credit: Gaskell produced the shape-model of Itokawa used [3].

3. System design

The mission is feasible with only an impactor and a program of ground-based observations providing information on the physical effects of the impact (Concept 1). However, the mission can be expanded to suit a range of budgetary options (see Fig. 2): the mission return can be greatly increased by adding an ejectable flyby subunit that observes the impact event itself and the resulting ejecta cloud in detail, while also acting as a relay node for data acquired by the impactor during the last minutes before impact (Concept 2). With this addition, a major part of the objectives of a reconnaissance probe can be achieved without the need for a separate, independent second deep-space mission. The expanded mission has features similar to the Deep Impact mission, which was a two-part spacecraft that separated before impact into an impactor and a flyby imager. The flyby imager slowed down slightly to observe the impact and then looked back to observe the ejecta cloud. It would also be possible to add small subunits (here named Chasers) to the mission (Concept 3). The Chasers would be ejected during the impactor's final approach, and would provide close up views of the impact, which is similar to the configuration of the 2009 LCROSS mission to impact the lunar southern pole. The chasers would use the flyby module for data buffering and relay to Earth.

3.1. Flyby subunit

For mission Concepts 2 and 3 the flyby subunit is released in the final-approach phase with a trajectory offset to perform a safe but close flyby of the asteroid to provide for good resolution images with sufficient time delay to observe the impact (see Fig. 2). The subunit carries monitoring instrumentation and a communication link to Earth. To function as a relay node for the other units it has inter-spacecraft communications, and data storage capability to allow a post-flyby data downlink. The flyby unit must handle high incoming data rates, albeit only for a short time interval around impact.

One of the main challenges of the flyby subunit is the imaging geometry necessary to image the impact from a close flyby

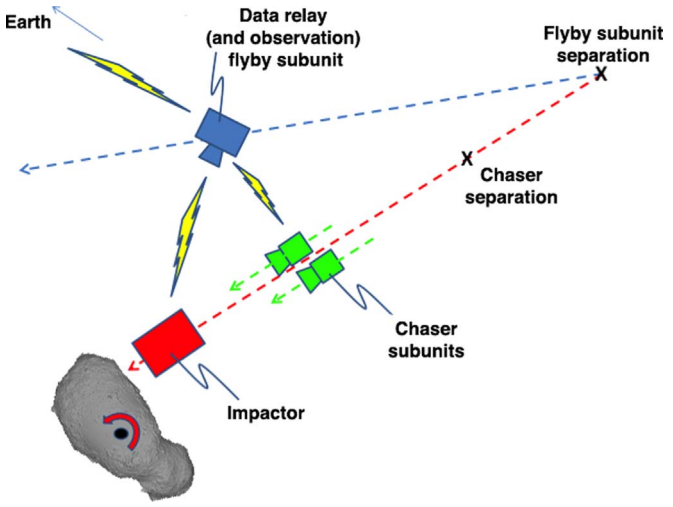

Fig. 2. Subunits' release sequence. Depending on the budget, there are options for different mission scenarios: 1) impactor, 2) impactor+ejectable flyby subunit, and 3) impactor+ejectable flyby subunit+Chaser subunits.

trajectory. For the current baseline geometry (flyby distance of 20 km) the target azimuth and azimuth rate gives a peak rate of 25 °/s and a non-constant rate profile. Tracking the target via an attitude maneuver of the flyby subunit is challenging. A solution currently deemed more feasible is the use of a targeting mirror on a fixed-attitude platform. The actuation of the tracking mirror can be implemented in an open-loop fashion or using image based tracking. The latter is more challenging in terms of development but more robust to uncertainties in predicted flyby geometry.

3.2. Chasers

For mission Concept 3, the Chasers will be released at a later stage, after all major trajectory corrections have been performed, in order to follow close behind the impactor and observe the impact and the early plume evolution at close range. The vantage point of the Chasers inside the main ejecta cone (assuming that the majority of ejecta are escaping on a ~45° cone mantle [4]) may also allow observation of initial crater formation. Mission planning can ensure that at the time of impact the sun illuminates the target area through the ejecta cone. The data from the two Chasers is transmitted to the flyby subunit where it is stored and re-transmitted to Earth either in near-real-time or with a delay. The fate of the Chasers is somewhat uncertain: they could be hit by plume debris, become impactors on the asteroid themselves, or miss the asteroid altogether. In any case, it should be possible to determine their fate via the data acquired by the Chasers and the time of link termination between the Chasers and the flyby subunit, which is relevant for the calculation of the total momentum transferred to the asteroid.

In the interests of cost efficiency, we assume to start with a very simple attitude and orbit control system, and propulsion subsystem, for the essentially passive subunits (single-gyro stabilized attitude, a single cold-gas thruster for delta-V). The strategy has some similarity to the one already employed in the Rosetta/Philae lander concept. A consequence of the simplicity is that the Chasers will not be able to make trajectory corrections after release: hence a late release is necessary to keep on target. Further, the camera field of view must be able to accommodate a certain amount of uncertainty in relative target location. However, the later the release, the more delta-V is required to give sufficient time-delay for the observations. Determination of the optimal release time will require a careful trade-off between these aspects.

3.3. Impactor

The impactor concept is thought to uses the Lisa Pathfinder propulsion module, plus a customized mission module housing all other spacecraft functionality, including the camera for terminal visual navigation and all equipment necessary to perform guidance, navigation, and control for final approach. The Lisa Pathfinder propulsion module is modified by an additional propulsion branch that feeds the thrusters needed for final approach control. The thrusters are spread out over the propulsion module and the mission module to provide full 6-degree of freedom control authority. The use of the existing Lisa Pathfinder propulsion module is attractive in terms of development cost.

The impactor navigation camera also functions as the primary payload instrument, collecting target images up to the time of impact. Further, the impactor features a communication link to the flyby unit to transmit final approach data, which is stored there and later transmitted to Earth. As an option to enhance mission redundancy, the impactor could additionally have a direct Earth communication link.

4. Target asteroid

For this mission the most important condition for target asteroid selection is that the change in rotational period should be measurable from Earth-based telescopes in the years following the impact. It follows that the selected target should be at most around a few hundred meters in diameter, and its orbit and lightcurve amplitude should allow Earth-based telescopes to measure the change in rotational period in a reasonably short time.

While it is not essential, the lack of an in-orbit reconnaissance spacecraft to observe the impact and characterize the asteroid before and after will reduce the scientific return. Choosing a previously visited asteroid as a target, however, would partially compensate for this since some scientific context for the mission would already be available. In addition, detailed a-priori knowledge of the asteroid geometry is critical to the precision targeting that this mission calls for. Possible targets in the few hundred meters size class include 25143 Itokawa (the Hayabusa I target, 2005), 101955 Bennu (the Osiris-Rex target, 2018) and 162173 Ryugu (the Hayabusa II target, 2018). Of these 3 asteroids only Itokawa has been visited to date. Fortunately, Itokawa's elongated shape (see Fig. 1) is highly advantageous for the mission proposed here because it facilitates accurate measurement of its rotational period from lightcurves. Itokawa's rotational axis is practically perpendicular to the ecliptic plane (−89.66° in ecliptic coordinates [5]), making observations of the lightcurve possible whenever it is close enough to Earth. The JAXA spacecraft Hayabusa visited Itokawa in 2005–2007 to characterize it and return samples from the surface to Earth [2]. For the above reasons Itokawa has been chosen as the target for this kinetic-impactor demonstration mission study.

A further attractive feature of using Itokawa as a target is that it gives rise to launch opportunities every 3 years (see Section 7), providing high programmatic flexibility.

5. Impact analysis

5.1. Estimating the effect of an impact on Itokawa

The impulse moment transferred to the asteroid from an impact depends on the mass, m_i and velocity vector, $\mathbf{v_i}$, of the spacecraft, as well as how much material, m_e, is ejected by the impact and the velocity vector, $\mathbf{v_e}$. The total impulse moment in the direction of flight due to the impact, $(m_i\mathbf{v_i}+m_e\mathbf{v_e})$ can be written as $\beta m_i\mathbf{v_i}$, where β is called the momentum enhancement factor or β-factor.

The expected change in rotational period as a consequence of the deflection mission can be estimated based on angular momentum conservation. The change in rotational frequency is given by

$$\omega_z-\omega_{z0}=[1+(\beta-1)\cos\phi]m_i v_i d\sin\theta/I_{zz}. \quad (1)$$

Assuming any change in the moment of inertia around the Z-axis, I_{zz}, following the impact being negligible. See Fig. 1 for an explanation of most of the symbols.

To roughly estimate the change in rotational period, it is assumed that there is no enhancement to the change in angular momentum from ejecta, $\beta = 1$, which in most cases should be a significant underestimation. Taking m_i=625 kg, v_i=8 km/s (the worst-case scenario values from the 5 mission trajectories – see Section 7), $d\sin\theta$,=100–225 m (from the optimal impact points on Itokawa – see Section 5.2.3), $I_{zz}=7.77^{*}10^{8}$ km^2 kg [6] and the rotational period, T_0=12.132370 h [6], Eq. (1) gives a change in the

rotation period of Itokawa (T_z–$T_{z0}=2\pi/\omega_z-2\pi/\omega_{z0}$) between 3.3 and 7.3 min, which is 0.5–1% of Itokawa's period. This result reflects the lower limit in the expected change of period. In the case of ejecta production the resulting values could possibly more than double.

5.1.1. Spherical versus elongated target

In the case that a more spherical asteroid, such as Bennu or Ryugu, would be chosen as the target for the mission, a few further issues have to be considered:

The main challenge with a spherical asteroid is measuring the rotational period precisely from lightcurve data. Bennu and Ryugu have lightcurve amplitudes of only ~0.17 [7] and ~0.12 magnitude [8] respectively, while that of Itokawa is ~1 magnitude [9]. However, the precision to which the change in rotational period can be measured also depends on the asteroid's mass, orbit and rotational axis compared to the line of sight to Earth.

The main benefit of a spherical target asteroid is its relatively low moment of inertia, which makes it easier to change its rotational period. If Itokawa were spherical it would have half the moment of inertia. However, the rounded surface will cause the net direction of the ejecta momentum to have an angle, ϕ, to the impact direction, which will reduces the momentum enhancement achieved from the ejecta, the $(\beta-1)\cos\phi$ term. One of the benefits of Itokawa's shape is that it is possible to choose an impact site such that the net direction of the ejecta, ϕ, is close to 0, while presenting a relatively long lever arm.

5.2. Optimal impact point

To find the optimal point to impact Itokawa several effects have to be taken into account. Firstly, it is important to avoid a significant shape change arising as a consequence of the impact, as this would change the moment of inertia of Itokawa and, consequently, the rotation period, complicating measurement of the momentum enhancement factor.

5.2.1. Head or body?

Since Itokawa is expected to be a rubble pile asteroid with unknown cohesion strength, it seems prudent to choose an impact site on the largest of the two apparent main components, meaning targeting the “body” instead of the “head”.

5.2.2. Eastern or western side of the body?

The boulders on Itokawa are aligned in such a way that they must have been moved by impact-induced vibrations [10,11], therefore impacting close to large boulders should also be avoided in case they move and change the moment of inertia of the asteroid. Comparing the western side of the “body”, which includes the large boulder Yoshino-dai (one tenth of the length of Itokawa) in the vicinity of a natural impact site, with the eastern side that offers a large flattish area called Linear having a surface tilt favorable for maximizing the impact torque, leads to a preferred impact site on the eastern side of Itokawa's “body” (see Fig. 1).

5.2.3. Optimal impact point on the eastern side of the body

To find the optimum impact location on Itokawa we have performed a quantitative analysis of the expected torques created by the impact in a grid of potential target areas.

Gaskell Itokawa shape model, V1.0 [3] was used to generate a map of surface normals (see Fig. 3). The surface normals were then used as a proxy for the direction of the ejecta momentum, since the net direction of ejecta is in most cases centered on the normal to the surface [12]. The impact direction is assumed to be along the model's *Y*-axis as this is perpendicular to the longest axis of Itokawa. The *Z*-axis of the shape model is practically identical with

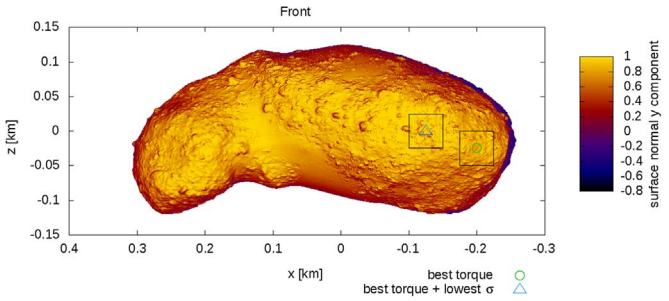

Fig. 3. Optimum impact locations. Map of *y* components of the surface normal vectors on Itokawa's eastern side. Marked areas indicate the best impact locations with respect to optimum torque and optimum torque with lowest variance.

Itokawa's axis of rotation. Therefore the *X*-component of the impact point is the lever arm of the impact torque.

Assuming an impact location uncertainty of 25 m, the *X*–*Z* surface was scanned and 50-meter squares were drawn at 25 m intervals. Within each square the mean, A_y, and variance, σ_y, of the *Y*-components of the surface normal vectors were calculated. The relative torque was then calculated by taking the *X*-component of the center point, $|r_x|$, (the lever arm of the torque) and multiplying it by A_y. If, however, the variance of the surface normals within a square is large, then the risk of hitting a surface element with a very different A_y than the mean is greater. To account for this, relative torque is divided by the variance of the normal: $|r_x|\ A_y/\sigma_y$.

The best torque position ($|r_x|\ A_y$) was found to be (−200 m, 129 m, −3 m) in the Gaskell model [3] (see Fig. 3) and the angle between the (negative) impactor vector and the average net ejecta vector was less than 21.5° (1σ variance) in the square.

The largest ratio torque/variance ($|r_x|\ A_y/\sigma_y$) was found at (−125 m, 142 m, 0 m), having a 1σ variance of less than 19.8° (see Fig. 3). For this proof of concept this more cautious choice has been chosen. However for an actual mission the location of the optimal torque might end up being targeted instead, due to the 75 m longer torque lever arm and that the variance is almost the same in the two cases.

The optimal impact location depends on the precise size of the spacecraft guidance, navigation and control system uncertainty, as that changes the size of the squares used in the calculations. The precise optimal locations will also shift slightly, if the impact vector is not exactly aligned with the *Y*-axis. Test calculations indicated however, that this variation is of the order of the guidance, navigation and control system uncertainty radius of 25 m. Deviations in the *X* and *Y*-direction will cause a change in torque lever arm. In Section 5.1 the lever arm length was varied between 100 and 225 m, which were shown to give a change in the rotation period of between 3.3 and 7.3 min in the example given, both of which are easily observable from Earth. Due to the primary rotational axis being the *Z*-direction, variation in the impact position in the *Z*-direction can cause the asteroid to tumble, the amount of which depends on the distance from the equator and the angular momentum transferred to the asteroid. This could give a secondary measurement of the $\boldsymbol{\beta}$-factor, however investigation is needed to compare the added benefit with the uncertainty added due to uncertainty in the moment of inertia in the *X*- and *Y*-axis.

6. Uncertainty in the measurement of the β-factor

6.1. Motivation

The largest uncertainties in the angular momentum transfer efficiency originate from the fact that very little is known about

the internal structure of Itokawa, and, by extension, its moment of inertia. Despite extensive Hayabusa mission data, there remain uncertainties in the precise location of the rotational axis of Itokawa. In their calculation of its moment of inertia Scheeres et al. [6] assumed a homogeneous mass distribution. However, the predicted spin-up of Itokawa of 0.2–0.4 s/yr, due to the asymmetry of the reaction forces of photons reflected and re-emitted from an irregular surface (the YORP effect [13]) was not confirmed by lightcurve data; rather, a decrease of $\sim$0.045 s/yr between 2001 and 2013 was established instead [10]. The discrepancy means either that the YORP effect is not fully understood [e.g., [14]], or that wrong assumptions/values were used in the predictions. Lowry et al. [10] propose a heterogenic density distribution, with the "head" of Itokawa having a density 1.63 times higher than that of the "body", in order to reconcile the observed spin-down with the predictions of the YORP effect. The change in the mass distribution has the effect of moving the center of mass and rotation axis $\sim$21 m towards the head. Taking this distribution as an extreme case, the possible variation of the moment of inertia is computed by using the *N*-Body code PKDGRAV [15,16].

6.2. N-Body simulation

Using 450,000 spheres with a power law distribution of sizes (ratio of largest to smallest:10/7, slope: -2.5), their collapse was computed under mutual self-gravity in free-space using PKDGRAV and the soft-sphere discrete element method [17] as the contact law. Once the collapsed ensemble of spheres had settled into a large sphere, small overlaps were removed entirely by shrinking each particle's radius by half its maximum overlap. A 3+million-facet Itokawa shape model [3] [Fig. 4 (left)] was then used to carve the collapsed sphere into the detailed shape of Itokawa [Fig. 4 (right)]. This model of the body was then scaled such that the longest principal axis was 555.8 m.

6.3. Results of the N-body simulation

The results for the two cases of density distribution and their respective moments of inertia are as follows:

1) Assuming a homogeneous density distribution, the moment of inertia tensor was computed. Those components representing the moments around the major, intermediate, and minor axes (x, y, and z, respectively) are: $(I_{xx}, I_{yy}, I_{zz})/M_{ito}=(6.25\times10^{-3}, 2.04\times10^{-2}, 2.15\times10^{-2})$ km^2, where M_{ito} is the entire mass of the body. This estimate of the moment of inertia around the principal axis of greatest inertia, I_{zz}, (taken to be the axis of rotation) is within 1% of the estimate given by Scheeres et al. [6].
2) Also calculated was the inertia tensor of an Itokawa with a density distribution characterized by having a head/body density ratio of 1.63, where the "head" is defined as the material at positions $x>150$ m (see Fig. 3), and material at positions $x\leq150$ m as the "body." Incorporating this into the above PKDGRAV Itokawa model (Fig. 4 (right)) shifts the center of mass by (20.6 m, 1.1 m, -2.0 m) with respect to the homogenous distribution's center of mass in the Gaskell model, in agreement with the work of Lowry et al. [10]. This distribution reorients the principal axes only slightly (about 1.6° for the major axis, and about twice this value for each of the other two) and gives moments of inertia around the X-, Y-, and Z-axes of $(6.06\times10^{-3}, 2.27\times10^{-2}, 2.36\times10^{-2})$ km^2 M_{ito}, respectively. This represents a 10% increase in the moment of inertia around the principal minor axis, I_{zz} (presumed rotation axis), when compared to a homogenous body.

The change in the presumed location of the rotation axis by 20.6 m towards the more dense "head," makes the torque lever arm at the impact point (discussed in Section 5.2.3 for the heterogeneous case 17% longer for the optimal torque/variance impact point and 10% longer for the optimal torque impact point. However, the increase in torque is largely mitigated by the 10% larger moment of inertia. Inserting these new values into formula (1) shows that, even with this extreme case of density inhomogeneity, the spin-up effect $(\omega_z-\omega_{z0})$ only increases with 0–7% compared to the homogeneous case. We would therefore expect a difference of less than 7% in the calculated β-factor. The β-factor can therefore be measured to a high precision with this proposed NEOTωIST mission, despite uncertainties in Itokawa's moment of inertia and rotation axis.

7. Trajectories

Trajectories have been computed with departure dates from the 1st of January 2020 to the 31st of May 2036, using a VEGA launcher model with the Lisa Pathfinder propulsion module, which remains attached to the impactor. The resulting trajectories have been ranked according to a figure of merit (FoM) defined as a weighted linear combination of the variables of interest.

The FoM (Eq. (2)) allows maximizing a combination of the spacecraft arrival mass (m_{PL}), and the impact impulse

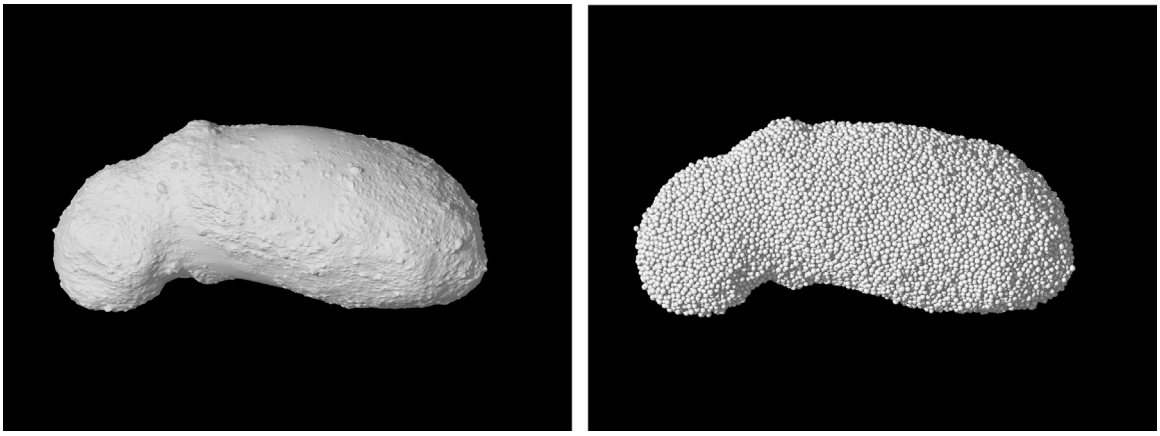

Fig. 4. Topographic and n-body model of Itokawa. Left: image of Itokawa rendered using the detailed topographical dataset from Gaskell et al. [3], interpreted by subroutines in the software package PKDGRAV and ray-traced with the Persistence of Vision Raytracer (POV-Ray). Right: region of spherical rubble pile carved out by this shape model (N=61,601).

perpendicular to the target spin axis (I_p) and minimizing the transfer duration (T_f), the number of Earth flybys $N_{FB} \leq 2$, and Itokawa's apparent magnitude from Earth at impact (m_{app}), which should be brighter than 21.1. All the factors in Eq. (2) are defined to reach an approximate maximum value of 1 (the variables involved add or subtract depending on if it is a term that needs to be maximised or minimised), which are multiplied by weights such that all terms add to 1. Therefore, the maximum value that the FoM can reach is approximately 1. It was also a constraint that the arrival velocity (V_{arr}) should be between 5–9 km/s, the departure declination should be between -5 and $+5°$, the arrival solar phase angle should be $<75°$ and the Earth should be within the line of sight of the impact point at impact.

The FoM is defined as:

$$\mathrm{FoM} = w_1\frac{m_{PL}-300\ \mathrm{kg}}{170\ \mathrm{kg}} + w_2\frac{I_p-2500\ \mathrm{kN\ s}}{3500\ \mathrm{kN\ s}} + w_3\frac{1200d-T_f}{1200d} + w_4\frac{2-N_{FB}}{2} + w_5\frac{21.1\ \mathrm{mag}-m_{app}}{5\ \mathrm{mag}} \quad (2)$$

with the set of weights $w=(20\%, 40\%, 10\%, 10\%, 20\%)$. The precise weights were determined based on prioritization of the parameters.

To generate mission trajectories from Lambert arcs a branch-and-prune algorithm was used with two or less Earth swing-bys. Swing-bys of Venus and Mars were also considered in early stages of the mission analysis but discarded because good solutions could be found without, thus eliminating the extra thermal design constraints.

The feasible trajectories showed tightly clustered arrival dates near those of the Itokawa periapsis. This is a result of the nearly 2:1 relation between the Itokawa orbital period and its synodic period with Earth. The generated missions were thus divided into five groups, arriving near the 2024, 2027, 2030, 2033 and 2036 perihelia, for ranking. The figures of merit were calculated and the mission with the maximum FoM was declared the "best solution" for each of these groups and the characteristics of the trajectories are summarized in Table 1.

On the assumption that a single spacecraft design will be performed, catering to the mass specification of one of those trajectories but usable in several of them, we also provide the linear impulse achievable by flying all the trajectories with the minimum spacecraft mass of all of them, which was 372 kg without the Lisa Pathfinder propulsion module mass for the 2030 impact point.

Table 1
Characteristics of trajectories with the best FoM values for each group. The quoted "spacecraft" masses refer to the achievable arrival mass of the all the subunits but without the Lisa Pathfinder propulsion module (LPF) upper stage (LPF dry mass is 268 kg). The impact linear impulse is computed with the actual arrival mass, which includes the LPF.

	Year of arrival group	**2024**	**2027**	**2030**	**2033**	**2036**
	Figure of merit (‰)	**643**	**622**	**661**	**947**	**838**
DEP and TRIP	Swing-bys	–	–	–	–	Earth
	Flight time (days)	581	942	589	95	503
	Earth V_∞ (km/s)	2.07	2.39	2.77	2.18	1.62
	Earth V_∞ declination (deg.)	0.1	0.3	2.7	4.7	−5.0
Arrival	Arrival V_∞ perpendicular to Itokawa axis (km/s)	7.99	8.45	8.86	8.97	8.92
	Arrival V_∞ declin. w.r.t. Itokawa equator (deg.)	4.5	5.4	5.2	2.6	2.5
	Spacecraft mass (w/o LPF, kg)	424	401	372	416	447
	Linear impulse normal to Itokawa axis (kN s)	5522	5653	5667	6135	6372
	Minimum mass linear impulse (kN s)	5107	5408	5667	5740	5704
	Sun-Itokawa-impactor angle at impact (deg.)	30	24	21	12	13
Observation	Earth-Itokawa distance at impact (AU)	0.95	0.68	0.39	0.09	0.25
	Itokawa apparent mag. from Earth at impact	21.0	20.6	19.5	16.0	18.2
	Earth-Itokawa-impactor angle at impact (deg.)	90	90	90	74	42
	Solar phase angle at impact (deg.)	61	67	70	63	53
	Solar elongation at impact (deg.)	63	74	89	112	115

8. Post-mitigation risk analysis

A kinetic impact on the surface of Itokawa will not only change the spin state, it will also alter the asteroid's heliocentric orbit and Itokawa's nominal close approach distances with respect to the Earth. To make certain that the change in Itokawa's orbit would not endanger the Earth no matter what the outcome of the mission, a post-mitigation impact risk assessment was conducted. The uncertainties in Itokawa's orbit, β-factor, direction and magnitude of the ejecta momentum vector, impact date, in addition to the overall mission success probability, were all taken into account [18].

In order to investigate the influence of the combined impact and orbit uncertainties the extended line of variation sampling technique presented in Eggl et al. [18] was employed. The impact itself is simulated using 1000 possible system realizations along the weak axis of the uncertainty covariance matrix using orbital elements and covariances for Itokawa taken from the JPL small body database [19] to a ± 3 sigma linear line of variation. DE431 Planetary ephemeris data [20] were used to obtain positions and velocities of the major bodies in the dynamical model. The total impactor mass was assumed to range between 520 kg and 640 kg depending on whether or not all subunits launch correctly and hit or miss the target according to plan. An overall mission failure probability of 10% was assumed. Itokawa's mass range was set to $(3.51 \pm 0.104) \times 10^{10}$ kg [2].

In total 11 simulations were performed, where three cases per trajectory were investigated:

1) A non-deflection (untouched) case.
2) A nominal deflection success (i.e., without mitigation uncertainties).
3) A case containing all previously described uncertainties.

All cases were propagated up to January 1st, 2105 and the corresponding minimum encounter distance probabilities calculated.

The simulations show that in all the cases tested the impact threat to Earth, as represented by the Palermo Scale value, remained very small (around -8 in the logarithmic scale) [21], as the Earth minimum miss distance continued to be more than 10 lunar distances. In the worst-case scenario the minimum miss distance in the next 100 years was decreased by less than 0.003%.

In summary, from a planetary safety perspective all 5 trajectories are viable with a preference for early launch years.

9. Observation from ground

9.1. Angular momentum

Will a change in Itokawa's rotational period of approximately 4 min be measurable from Earth in the years following the

impact?

Itokawa has an absolute magnitude of $H=19.2$, and the apparent visual magnitude seen from Earth can be found in Fig. 5. In the years 2024, 2027 and 2030 the apparent magnitude will brighten to $m_v=19$ magnitudes, and in 2033 and 2036 to $m_v=16$ magnitude.

The uncertainty on the rotational period can be estimated by using [22]

$$\Delta P \approx U * P^2/\Delta T \quad (3)$$

where P is the period, ΔP is the precision of the period, ΔT is the time interval between first and last lightcurve observations, and U is the relative uncertainty in measuring the rotational phase from fitting the lightcurve. For an asteroid such as Itokawa with a lightcurve magnitude amplitude of 1 mag, the relative uncertainty when fitting the lightcurve is around 1/20 of the rotational phase for $m_v=20.5$ [Stefano Mottola, personal communication]. Since Itokawa is well observable for many years following the impact, ΔT can become very large and ΔP very small over time.

To estimate how well the period can be measured within a year of the impact, the impact times described in the Section 7 are used. Assuming access to a 2-m telescope, it should be possible to perform lightcurve observations down to an apparent magnitude of around $m_v=20.5$. ΔT is therefore the time interval between the first time the asteroid brightness is brighter than 20.5 (or the impact occurs) to the last time within the time span of a year.

For the trajectory with impact date in 2024, there are about 44 days from the first time Itokawa was brighter than 20.5 after the impact to the last time. In 2027, 2030, 2033 and 2036 there are 59, 249, 217 and 215 days respectively. With a larger telescope fainter apparent magnitudes can be reached, giving larger ΔT.

In the 2024 impact case an uncertainty of 0.4 min is obtained when using Eq. (3) for the first year after impact. With a change of 4 min in the rotational period, this precision is of the order of 10%, and should be good enough for our purposes for the first year. After the next apparition the uncertainty will be reduced to 1 s due to the large value of ΔT. For the potential impact dates in 2030, 2033, and 2036, the precision will be of the order of 3–5 s in the first year following the impact.

9.2. Linear momentum

The motivation for the NEOTωIST's concept is that measuring the β-factor from the change in the rotational period of the asteroid (due to angular momentum transfer from the impact) is significantly easier than measuring it from the change in the asteroid's heliocentric orbit (due to the linear momentum transfer from the impact). However as any additional constraints on the β-factor would be desirable, estimates for the Detection Signal-to-Noise Ratio (DSNR) of the change in the heliocentric orbit of the planned mission scenarios were studied, i.e., the ratio between the change in Itokawa's orbit and its orbit uncertainty (see Section 8 for details on the method) [18]. As expected, the calculated DSNRs are not very large (between 6 and 7). DSNRs of 6–7 may be sufficient for a detection of the deflection action, assuming the orbit uncertainty can be kept at the current level and Itokawa's semi-major axis is used as an observable. However, placing significant constraints on the β-factor would require larger DSNRs.

A significant reduction of Itokawa's current orbit uncertainty of ~400 m before and after the impact would be necessary to increase the DSNRs, some improvements might be possible with radar observations that would be feasible during the close flybys in 2033 and 2036. The theoretically achievable orbit uncertainty is limited by the uncertainties in the position of Itokawa's center of mass (~20 m). If it is possible to constrain the uncertainty of Itokawa's semi-major axis to 20 m, then DSNRs of 70–100 are possible, which may be sufficient to constrain the β-factor to a reasonable degree. However, as decreasing the orbit uncertainty by an order of magnitude via Earth-based observations is extremely difficult, independent calculations of the β-factor based on the changes in the heliocentric orbit is not expected.

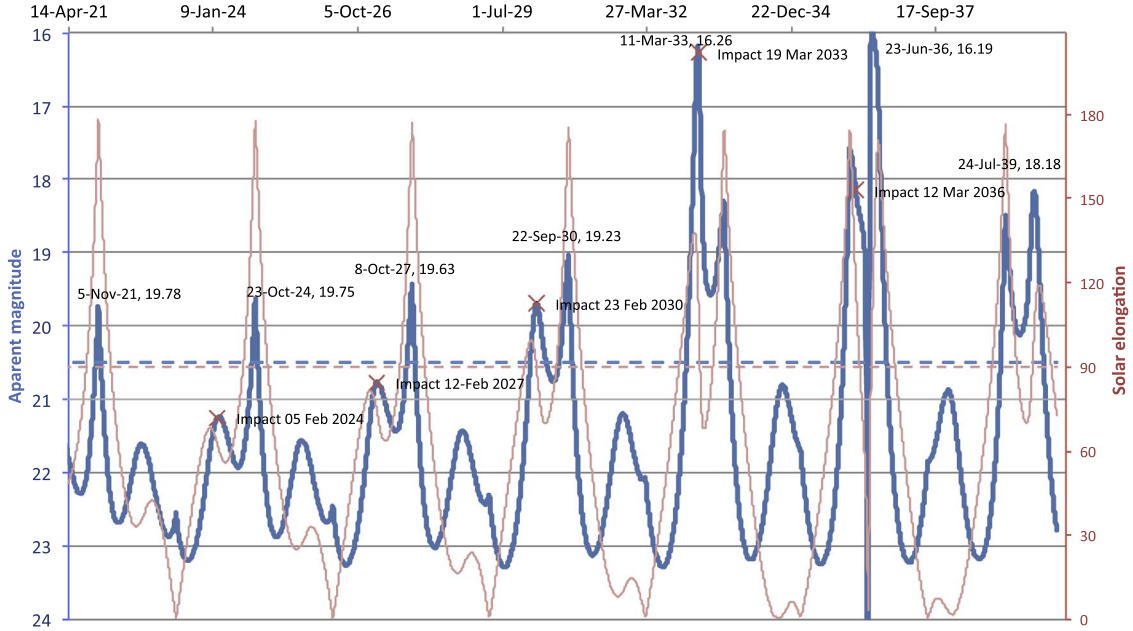

Fig. 5. Observability of Itokawa 2020–2040 The apparent visual magnitude of Itokawa in the period of 2021–2039 (dataset from JPL Horizons web service, 2015). The dashed blue line shows the apparent visual magnitude of $m_v=20.5$, which is around the limit of a rotation period measurement with a 2 m telescope. Using a larger telescope would allow the observations to continue to fainter apparent magnitudes, which would be beneficial especially in the case of missions in 2024 and 2027. During the close approach to the Earth in 2033 and 2036 it would be possible to observe Itokawa with radar, e.g. with the Arecibo and Goldstone facilities. The Sun–Earth-Itokawa angle is plotted as a thin red line (vertical axis on the right). We have assumed that observations will not be practical when Itokawa is less than 90° from the Sun as seen from Earth. (For interpretation of the references to color in this figure legend, the reader is referred to the web version of this article.)

9.3. The YORP effect

The YORP effect on the rotational period of Itokawa was found from lightcurve data between 2001–2013 to be only ~0.045 s/yr [10]. This value is about 6 orders of magnitude less than the changes from the impact, as discussed here, and therefore cannot complicate the analysis of the momentum impacted from the mission. Since the YORP effect is very shape-dependent, it may be instructive to re-measure and re-model the YORP-induced drift of the rotation rate after the impact to check for any unexpectedly large shape changes. The results could be compared with radar observations during the flybys in 2033 and 2036.

10. Conclusions

The aim of the NEOTωIST mission concept is to impact a previously-visited asteroid, e.g., Itokawa, thereby changing its spin rate and determine the efficiency of momentum transfer. NEOTωIST would also help to mature the technology required for a kinetic impactor mission. The mission would therefore represent a crucial precursor for a future space mission to deflect an asteroid by collisional means in an emergency impact-hazard situation. A preliminary analysis of the mission concept has revealed no major conceptual flaws. Our current judgment of the mission is that it constitutes an attractive option for a low-cost, high figure-of-merit kinetic-impactor demonstration and characterization mission. The main savings with regard to typical kinetic-impactor mission concepts (such as Don Quijote) result from dispensing with the rendezvous/observer spacecraft and associated launch and operations. Our impactor-only mission concept targets a known well-characterized object, where the net momentum transfer can be validated directly from Earth via post-mission telescope observations.

The augmentation of an impactor-only concept with co-flying subunits at final approach that observe the impact event at close range provides much of the information that an observer spacecraft would otherwise provide, but at a significantly lower cost. The technological capability that this constitutes is not only valuable for this demonstration mission, but might also be of significant benefit to other future missions.

The high mission return to cost ratio of the concept is also attractive in programmatic terms. Through appropriate selection of architectural options the mission cost can be adapted to a range of budgetary environments. Further, the mission geometry is such that launch opportunities occur every three years, which provides for a flexible program implementation timeline.

Acknowledgments

We would like to thank Dan Scheeres and Steve Chesley for useful discussions. The research leading to these results has received funding from the European Union's Seventh Framework Programme (FP7/2007-2013) under Grant agreement no. 282703 (NEOShield) and H2020- PROTEC-2014 - Protection of European Assets in and from space project no. 640351 (NEOShield-2).

References

[1] A.W. Harris, M.A. Barucci, J.L. Cano, A. Fitzsimmons, M. Fulchignoni, S.F. Green, D. Hestroffer, V. Lappas, W. Lork, P. Michel, D. Morrison, D. Payson, F. Schäfer, Acta Astronaut. 90 (2013) 80–84.
[2] A. Fujiwara, J. Kawaguchi, D.K. Yeomans, M. Abe, T. Mukai, T. Okada, J. Saito, H. Yano, M. Yoshikawa, D.J. Scheeres, O.S. Barnouin-Jha, A.F. Cheng, H. Demura, R.W. Gaskell, N. Hirata, H. Ikeda, T. Kominato, H. Miyamoto, A.M. Nakamura, R. Nakamura, S. Sasaki, K. Uesugi, Science 312 (2006) 1330–1334.
[3] R.W. Gaskell, J. Saito, M. Ishiguro, T. Kubota, T. Hashimoto, N. Hirata, S. Abe, O. S. Barnouin-Jha, D. Scheeres, NASA Planet. Data Syst. (2008).
[4] J.E. Richardson, J. Geophys. Res. E Planets 116 (2011).
[5] H. Demura, S. Kobayashi, E. Nemoto, N. Matsumoto, M. Furuya, A. Yukishita, N. Muranaka, H. Morita, K. Shirakawa, M. Maruya, H. Ohyama, M. Uo, T. Kubota, T. Hashimoto, J. Kawaguchi, A. Fujiwara, J. Saito, S. Sasaki, H. Miyamoto, N. Hirata, Science 312 (2006) 1347–1349.
[6] D.J. Scheeres, M. Abe, M. Yoshikawa, R. Nakamura, R.W. Gaskell, P. a Abell, Icarus 188 (2007) 425–429.
[7] C.W. Hergenrother, M.C. Nolan, R.P. Binzel, E.A. Cloutis, M.A. Barucci, P. Michel, D. J. Scheeres, C.D. D'Aubigny, D. Lazzaro, N. Pinilla-Alonso, H. Campins, J. Licandro, B.E. Clark, B. Rizk, E.C. Beshore, D.S. Lauretta, Icarus 226 (2013) 663–670.
[8] M.-J. Kim, Y.-J. Choi, H.-K. Moon, M. Ishiguro, S. Mottola, M. Kaplan, D. Kuroda, D.S. Warjurkar, J. Takahashi, Y.-I. Byun, Astron. Astrophys. 550 (2013) L11.
[9] S.C. Lowry, P. Weissman, M. Hicks, R. Whiteley, S. Larson, Icarus 176 (2005) 408–417.
[10] S.C. Lowry, P.R. Weissman, S.R. Duddy, B. Rozitis, A. Fitzsimmons, S.F. Green, M. D. Hicks, C. Snodgrass, S.D. Wolters, S.R. Chesley, J. Pittichová, P. van Oers, ASTRON 48 (2014).
[11] H. Miyamoto, H. Yano, D.J. Scheeres, S. Abe, O.S. Barnouin-Jha, A.F. Cheng, H. Demura, R.W. Gaskell, N. Hirata, M. Ishiguro, T. Michikami, A.M. Nakamura, R. Nakamura, J. Saito, S. Sasaki, Science 316 (2007) 1011–1014.
[12] D.E. Gault, J.A. Wedekind, Lunar Planetary Science Conference 9th, vol. 3, 1978, pp. 3843–3875.
[13] D. Rubincam, Icarus 148 (2000) 2–11.
[14] O. Golubov, Y.N. Krugly, Astrophys. J. 752 (2012) L11.
[15] J.G. Stadel, Thesis (Ph.D.), University of Washington, 2001, p. 21.
[16] D.C. Richardson, T. Quinn, J. Stadel, G. Lake, Icarus 143 (2000) 45–59.
[17] S.R. Schwartz, D.C. Richardson, P. Michel, Granul. Matter 14 (2012) 363–380.
[18] S. Eggl, D. Hestroffer, W. Thuillot, D. Bancelin, J.L. Cano, F. Cichocki, Adv. Sp. Res. 56 (2015) 528–548.
[19] R.S. Park, A. Chamberlin, 2015.
[20] W.M. Folkner, J.G. Williams, D.H. Boggs, R.S. Park, P. Kuchynka, IPN Progress Report (2014) 42–196, http://ilrs.gsfc.nasa.gov/docs/2014/196C.pdf.
[21] S.R. Chesley, P.W. Chodas, A. Milani, G.B. Valsecchi, D.K. Yeomans, Icarus 159 (2) (2002) 423–432.
[22] J. Torppa, M. Kaasalainen, T. Michałowski, T. Kwiatkowski, A. Kryszczyńska, P. Denchev, R. Kowalski, Icarus 164 (2003) 346–383.

Line Drube is a planetary scientist educated at the University of Copenhagen, UCLA, and the International Space University. During her Ph.D. she was a science team member and downlink engineer on the Phoenix Mars mission. Since 2012 she has worked at the German Aerospace Center's Institute of Planetary Research researching the physical properties of near-Earth objects (NEOs) and NEO deflection demonstration missions. As a member of the German delegation to UN's COPUOS she has worked on the recommendations from Action Team 14 and the SMPAG for a coordinated international response to the NEO impact threat.

Prof. Alan W. Harris has held positions at the Max Planck Institute for Astronomy in Heidelberg, Germany, and at the Rutherford Appleton Laboratory, UK. He is now a Senior Scientist at the German Aerospace Center's (DLR) Institute of Planetary Research in Berlin, and holds an Honorary Chair at Queen's University Belfast, UK. He has served as Chairman of ESA's NEO Mission Advisory Panel and was a member of ESA's Solar System Exploration Working Group (2010–2012). He led the 13-partner, 5.8-million-euro, European Commission's NEOShield project. In recognition of his research the main-belt asteroid numbered 7737 was named after him in July 1999.

Kilian Engel graduated from the Technical University of Munich with a Masters of Aerospace Engineering. He did his thesis on a small-sat earth observation mission at Stellenbosch University in South Africa. Kilian has been extensively involved in the Summer Program of the International Space University, as a student, lecturer and academics program coordinator. Other experience includes a two-year trainee program with the European Space Agency. Currently, Kilian works on future mission concepts in the Program Department of Airbus Space Systems. Next to his professional interests he enjoys languages and travel, all manner of outdoor activities, and economics and finance.

Dr. Albert Falke is one of the first Ph.D. students to work on the Stuttgart Small Satellites Program (Institute of Space Systems, Universität Stuttgart). After his graduation he joined Airbus DS in Friedrichshafen, Germany, and contributed to several spacecraft implementation projects. Later he switched to the Future Programs Department where he was leader of, or contributor to, some space studies for the European Space Agency. Furthermore, in his responsibility for Small Body Missions Programmatics he led the company's activities within NEOShield. He is now project coordinator of NEOShield-2 and local project manager.

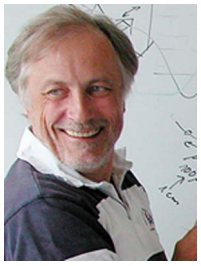

Ulrich Johann is presently head of department for future space science and earth observation mission and program developments at Airbus DS in Friedrichshafen, Germany. Besides internal scientific consultancy, he has led or system engineered many mission and instrument industrial studies and technology developments. Previously, he has been industrial project manager for the LISA- Pathfinder instrument as well as an associate professor of physics at the University of Illinois at Chicago, USA. He received his Ph.D. (Dr. rer. nat) in experimental and theoretical laser/rf spectroscopy of free atoms in 1981 after studying physics and astrophysics at the University of Bonn, Germany.

Siegfried Eggl, upon completion his master degree in astronomy, 2008 and one in physics, 2009 at the University of Vienna, Austria, Siegfried Eggl continued with a Ph.D. in the field of applied celestial mechanics, which he finished in 2013. Since then he has been working as a post-doctoral associate at the Institute for Celestial Mechanics and Ephemeris Computation (IMCCE) of the Observatoire de Paris, France. His research is mainly focused on asteroid deflection simulations and impact monitoring for the European Commission's NEOShield and NEOShield-2 projects, but several international collaborations target exoplanetary science as well.

Juan L. Cano is an Aeronautical Engineer graduated in 1994 at the Technical University of Madrid, Spain. Between 1995 and 1997 he enjoyed a grant at ESA/ESTEC on the Aerothermodynamics Section participating in several studies. He then moved for two years to the Mission Analysis Section at ESA/ESOC in Germany where he did contribute to the SMART-1 mission. Back to Spain he was co-founder of DEIMOS Space in 2001 where he has been involved in or managed many ESA projects, several of them related to interplanetary missions and NEO missions as Don Quijote, A-Track, Proba-IP, SysNova, etc, and lead DEIMOS contribution to NEOShield and Stardust.

Javier Martín Ávila is an Aeronautical Engineer graduated in 2012 at the Technical University of Madrid (Spain). Since then he has worked at DEIMOS in the field of mission analysis, where he has been mainly involved in the NEOSHIELD project (development of some NEO deflection tools) and other interplanetary missions like PhSR in its current and previous stages (PHOOTPRINT study). He has also collaborated in Earth-centric projects such as Proba-3.

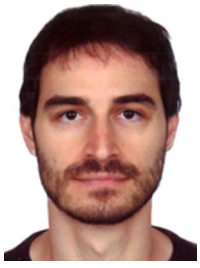

Stephen R. Schwartz is currently a post-doctoral researcher at the Observatoire de la Côte d'Azur in Nice, France, exploring the momentum transfer efficiency related to kinetic impactor mitigation missions to hazardous asteroids and the ejecta fate resulting from such impacts. After having received his Ph.D. in Astronomy from the University of Maryland, he performs analytical and numerical simulations under the auspices of the NEOShield project. As a planetary scientist, his expertise is in numerical simulations of granular dynamics in the intra-Solar System environment.

Dr. Patrick Michel is a CNRS Senior Researcher where he leads the Lagrange Laboratory planetology team at the Côte d'Azur Observatory, France. He is the European Advisory Team lead of the AIDA project under study by ESA and NASA (kinetic impactor test on the binary asteroid Didymos). He is co-I on NASA OSIRIS-REx and JAXA Hayabusa-2 sample return missions. He belongs to the Science Program Committee of CNES, the NEOShield-2 European Consortium and the International Asteroid Warning Network. He was awarded the Carl Sagan Medal 2012 (Division of Planetary Science, AAS), the Prize Paolo Farinella 2013 and the asteroid (7561) Patrickmichel.